Conceptual Design Review

Team 5 - Lamarvelous

AAE 451 - Senior Design; Aircraft Design Build Fly

By Nathen Carey, Aidan Doyle, Mike Flanagan, Max Gorlich, Jose Lara,
Ashwin Nathan, and Dhruv Wadhwa.

Table of Contents

Executive Summary

In this project, our team will design, build, and fly a remote-controlled aircraft around a preconceived flight course. There are several project milestones that we will utilize to show the progression of our design and share any and all major engineering decisions we make. This project milestone is the Conceptual Design Review (CDR), in which we will detail the final design of our aircraft. This includes the sizing, weights, structures, aerodynamics, propulsion, and stability/controls. In addition, we will be discussing the process in which we down-selected to our chosen design, the high level requirements we are using, the cost of the aircraft, the fabrication and manufacturing plans, and next steps.

High Level Requirements

A flight "score" is determined after flight tests based on the following equation:

$$\text{Score} = \text{Payload Weight} / \text{Time to Complete Course} \tag{1}$$

Many requirements are imposed on our design that come directly from the RFP, however, we also chose to develop our own requirements to guide us to build a well performing and high scoring aircraft for flight tests. The following list of requirements were those directly from the RFP:

- The aircraft shall be remotely piloted.
- The aircraft shall be propeller driven.
- The aircraft shall contain a fixed wing structure.
- The aircraft shall be capable of being launched by hand; there will be no rolling takeoff.
- The aircraft shall be capable of performing a belly landing.
- Aircraft shall at least have the range to complete three laps around a predetermined airfield course at McAllister Park.
- The aircraft shall be stored within a 30 in width x 30 in height x 60 in length storage volume.
- The aircraft wingspan shall be a maximum of 5 ft.
- After takeoff, the aircraft shall climb to a maximum altitude of 200 ft.
- The aircraft shall be easy to assemble, deploy and fly onsite; preflight construction time must be minimal.
- The payload and battery onboard the aircraft shall be easily and quickly swappable.
- The aircraft shall be stable under all flight conditions.
- The aircraft shall be easy to fly by a pilot external to the team.
- All teams shall use a standardized payload (weight and dimensions are equivalent per payload).
- All teams shall implement the same six-channel receiver and transmitter into their design.
- The maximum budget for materials and construction shall be 400$.

These requirements from the RFP gave our group a good starting point to begin a concept generation process. However, after design iteration and brainstorming, we realized we needed to further create and expand our requirements list to be more thorough and specific for the overall purpose of this design process. The following are requirements we felt were necessary to add, along with our rationale for their additions:

System, Performance, or Operational	Requirement	Rationale
System	The weight of the aircraft shall not exceed 30 lbs with payload.	Previous aircrafts were well under this weight. This will allow ease of handling compared to a larger aircraft.
Operational	The aircraft shall withstand and function in temperatures as low as 20 degrees fahrenheit.	Flight testing will occur during November, and although the weather will be hard to predict exactly, it would be better to prepare for colder weather.
Operational	The LiPo battery shall not be discharged below 3.2 V/cell. The team will decide on a minimum value to discharge at a later date.	LiPo batteries and performance will degrade when battery is discharged below this value
System	The aircraft shall include at least one unit of payload (one unit = 0.284 pounds, 1 inch steel cube with 5% manufacturing tolerances).	This is the minimum number of payloads required for this project.
System	The aircraft shall be relatively easy to construct and assemble.	We do not have experience building RC planes, so our concept should be simple and easy to construct
Performance	Aircraft C_{Do} shall be determined with the goal in mind to minimize parasitic drag during flight.	This value of parasitic drag coefficients will be used to form both our power constraint and our maneuvering constraint.
Performance	Aircraft L/D max shall be chosen to maximize our efficiency with the climb rate of our aircraft.	This value of $(L/D)_{max}$ values will be used to form our climb constraint.
Performance	Aircraft stall $C_{L,max}$ shall be at a value that allows the plane to maximize efficiency at stall speed.	The baseline $C_{L,max}$ value will be used to form our stall constraint.

Table 1: Internally derived requirements and rationales for their inclusion.

CONOPS

Our concept of operations has not had any major changes since SRR and SDR. We still plan the same mission around the airfield while carrying a payload. We plan to hand launch the aircraft, climb up to cruise altitude under 200 ft, complete 3 laps, and belly land. The only potential update is to our turning phase, where we are considering slowing down under our cruise speed to allow for greater control of the aircraft and a faster turn.

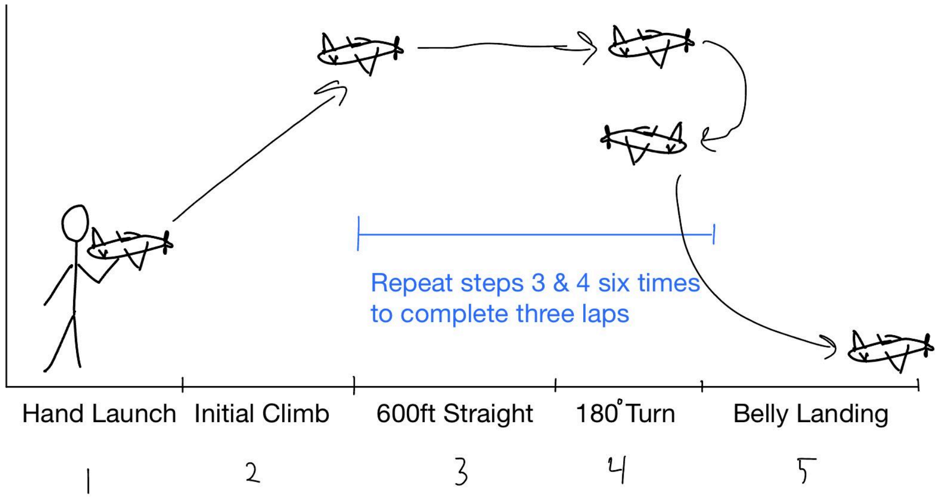

Figure 1: Concept of Operations

Best Aircraft Concept

After downselection, we decided that the best aircraft given our mission, requirements, CONOPS, and other criteria was a single engine, high wing puller aircraft. The following tables detail our design parameters and a comparison to a similar RC aircraft in the market now.

Design Parameters of Best Design	
Gross Weight	7.6 lbs / 50% increase is 11.4lbs
Payload	1.136 lb_f
Wing Loading	1.445 lb_f / ft^2
Wing Area	5.31 ft^2
Wing Aspect Ratio	4.71
Thrust to Weight ratio	1.31/ 0.87 for 50% increase in weight
Cost	$380.47

Table 2: Design Parameters

Criteria	**Baseline Aircraft Skynetic Shrike Glider** 	**Our Design** 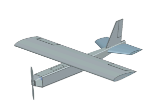
Cruise Speed	-	S
Payload	-	+

Ease of Construction	-	-
Controllability	-	+
Cost	-	-
Durability	-	+
Scores + S -	-	3 1 2

Table 3: Comparison to Baseline

Walkaround Chart

This is our final design showing a single engine puller with a high wing. Some other characteristics to note are the balsa structure for the fuselage, the lower wing spar for structure in the wing, the control surfaces on the wing and the tail, the ESC which is placed outside the fuselage for cooling reasons, the nose cone in front of the fuselage and the hatch to access the payload, motor and battery. All of these will be detailed further in the report.

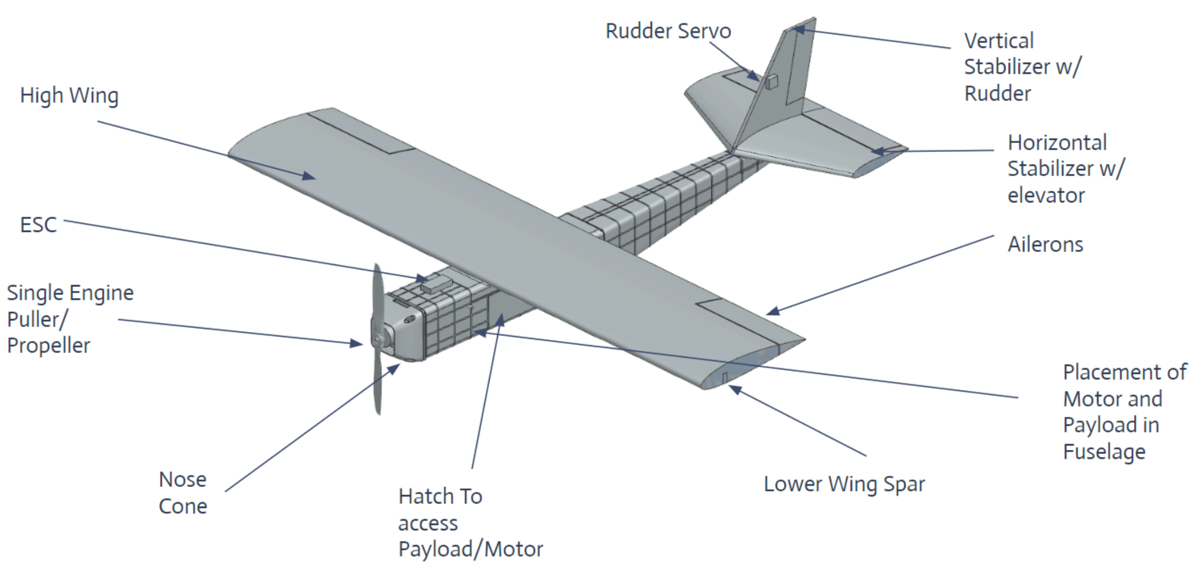

Figure 2: Walk Around Chart

Downselection

At the end of SRR+SDR after continuous iterations of brainstorming and doing the pugh's method, we were left with three aircraft concepts as seen below. The three designs were a High-Wing Twin Tractor, a Low-Wing Single Engine Puller, and a Blended Body Single Engine Pusher.

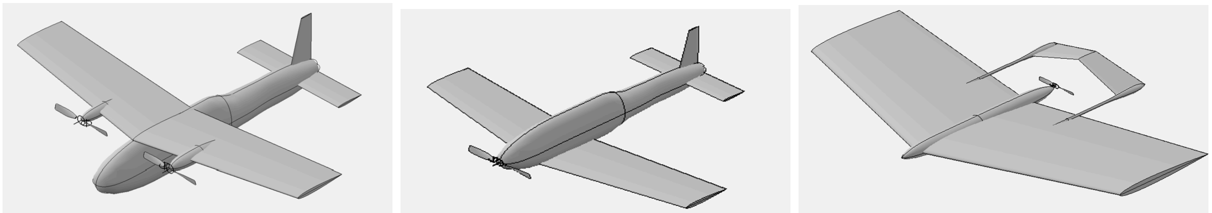

Figure 3: SRR+SDR Concepts

In SRR+SDR, we focused more on performance and mission goals. In CDR, as we approach manufacturing we must consider the extremely short time to build the plane and the budget. Therefore, our primary focus was on cost, design complexity, and ease of construction, while carefully weighing trade-offs with performance. We performed qualitative analysis to choose the best design while focusing on these attributes.

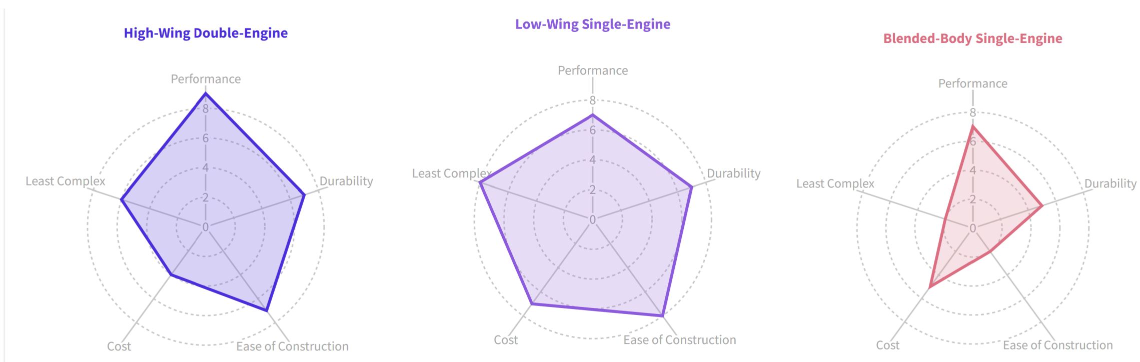

Figure 4: Qualitative Analysis of Final Concepts

<u>Combined View:</u>

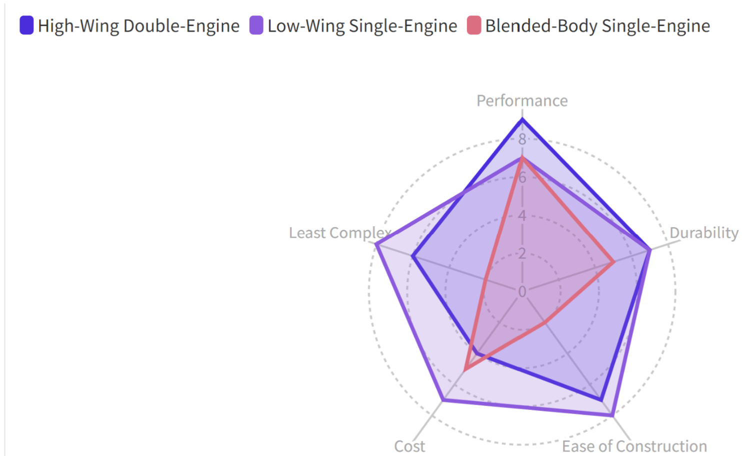

Figure 5: Qualitative Analysis of Final Concepts (Combined)

Looking at the diagram above it was clear to us that the blended body concept was simply not a concept we can pursue in this timeframe and budget and still have a high-performance aircraft. For that reason, the blended body was eliminated as an option for further consideration.

The other two designs that were left were the High Wing Twin Tractor and the Low Wing Single Engine Puller. The Low-Wing design did better on complexity, cost, and ease of construction than the

High-Wing design but did not perform as well as the High-Wing as that design has two engines that would lead us to have much higher speed and perform the mission faster.

To establish a compromise between the concepts we decided to merge the two concepts. Taking the single engine puller from the Low-Wing, and making it a High-Wing we are able to balance performance with cost, complexity, and construction.

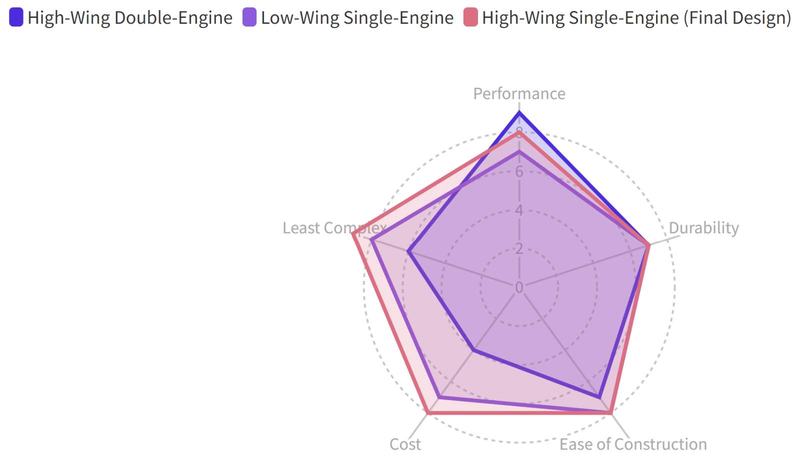

Figure 6: Qualitative Analysis including Final Design

Advanced Aircraft Description

The following are images of our CAD showing external layouts and internal layouts with dimensions including wing to nose, tail to wing, height, wing span and wing chord.

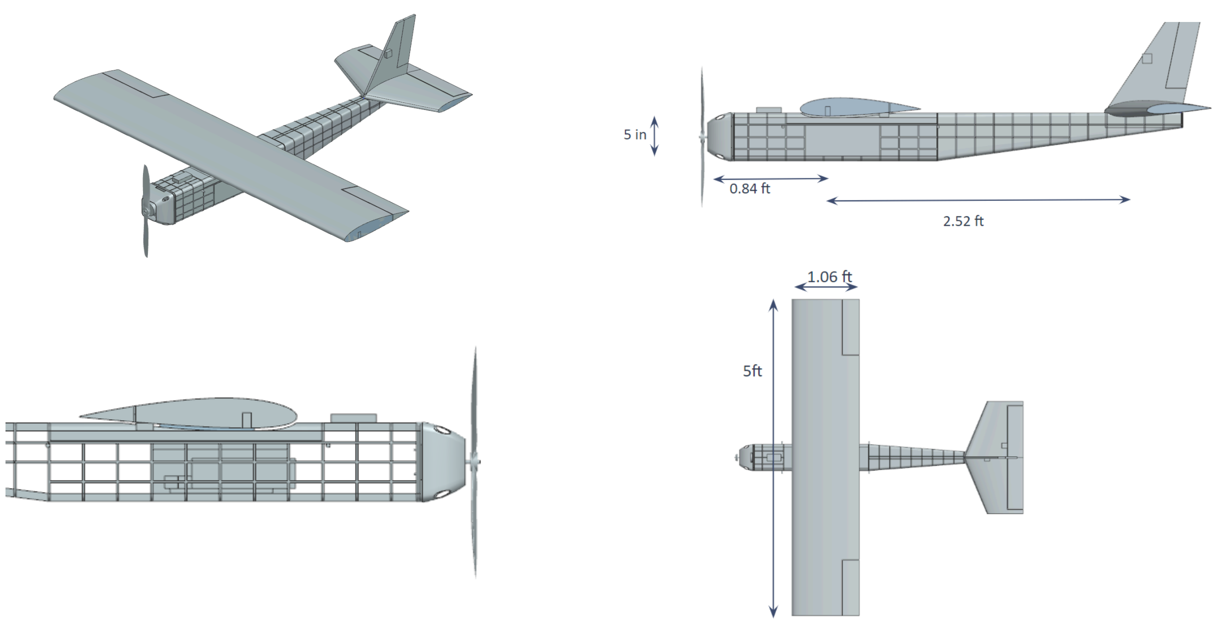

Figure 7: Various Views of Chosen Aircraft

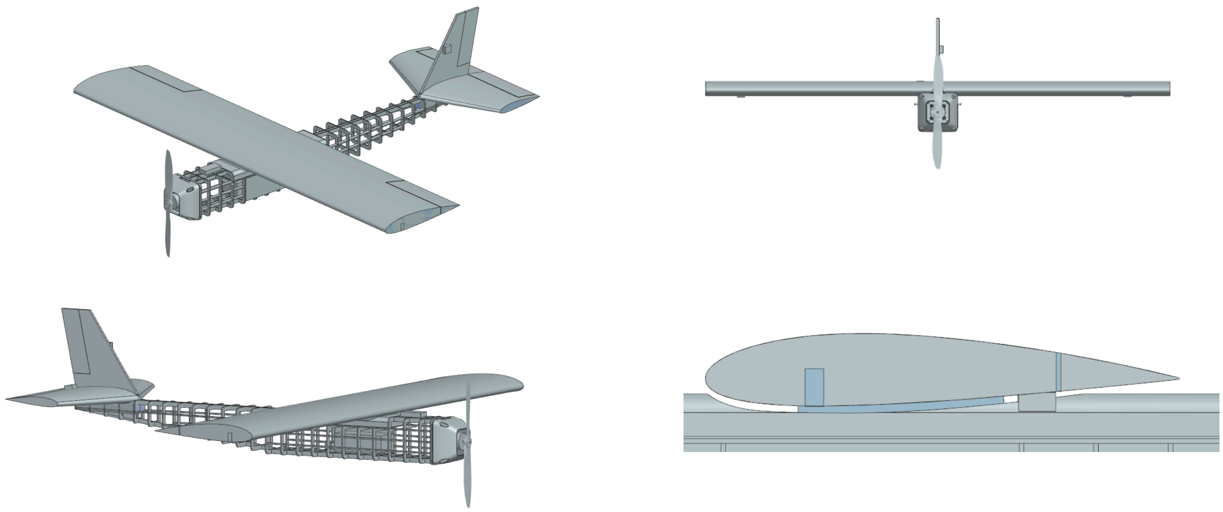

Figure 8: Other Angles of CAD

Structures and Weights

We chose to size our aircraft to carry 3 units of payload for the duration of the mission. This was a decision made early on with the help of the teaching team to ensure our estimated gross weight was below ten pounds. Our initial estimate with a 10% margin of error was 7.76 lb_f. As our design developed, we selected various systems that would be implemented on our aircraft (motor, battery, structural components, etc.) we were able to create a group weight estimate to tabulate our known weights. Rather than get a weight estimate using our CAD model, we decided that XFLR5 would be easier, and would allow for a visual representation of our weights (approximated as point masses) and our center of gravity. Presented below is our group weight estimate as well as our XFLR5 mass buildup view:

	Weights(lbs)	Location(ft)	Moment(ft-lbs)
Structures	3.41		7.42
Wing	1.76	1.68	2.96
Tail	0.66	4.5	2.97
Fuselage	0.99	1.5	1.49
Propulsion	1.08		0.39
Motor	0.88	0.18	0.16

ESC	0.13	0.84	0.11
Propeller	0.07	1.68	0.12
Equipment	0.29		0.96
Aileron servos	0.10	2.28	0.23
Elevator	0.11	4.2	0.46
Rudder Servo	0.05	4.1	0.21
Receiver	0.03	2.13	0.06
Total Empty Weight	4.78		8.77
Useful Load	2.21		3.41
Payload	1.14	1.58	1.8
Battery	1.07	1.5	1.61
Total Gross Weight	6.99		12.18

Table 4: Tabulated group weight statement

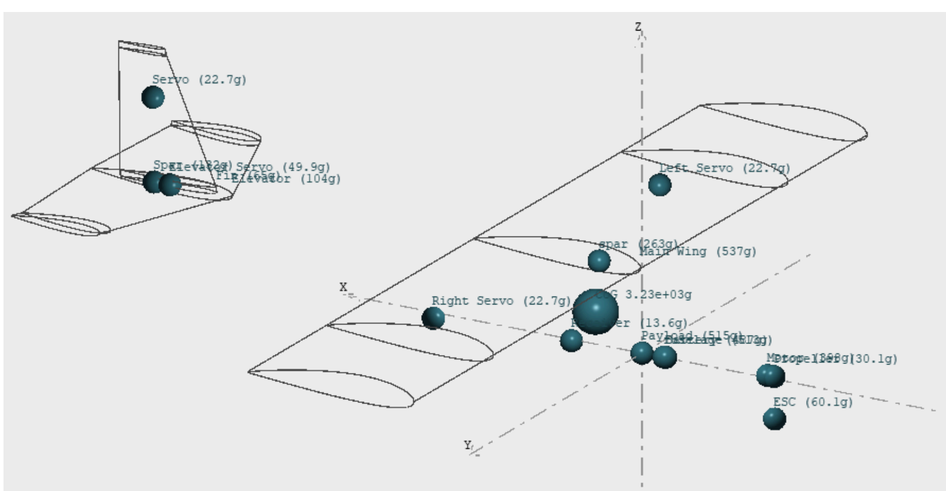

Figure 9: XFLR5 mass buildup view.

Using XFLR5, we were also able to instantly obtain our moments and products of inertia:

I_{xx}	I_{yy}	I_{zz}	I_{xz}
3.20 lb_m-ft^2	8.81 lb_m-ft^2	10.95 lb_m-ft^2	1.48 lb_m-ft^2

Table 5: Moments and product of inertia from XFLR5.

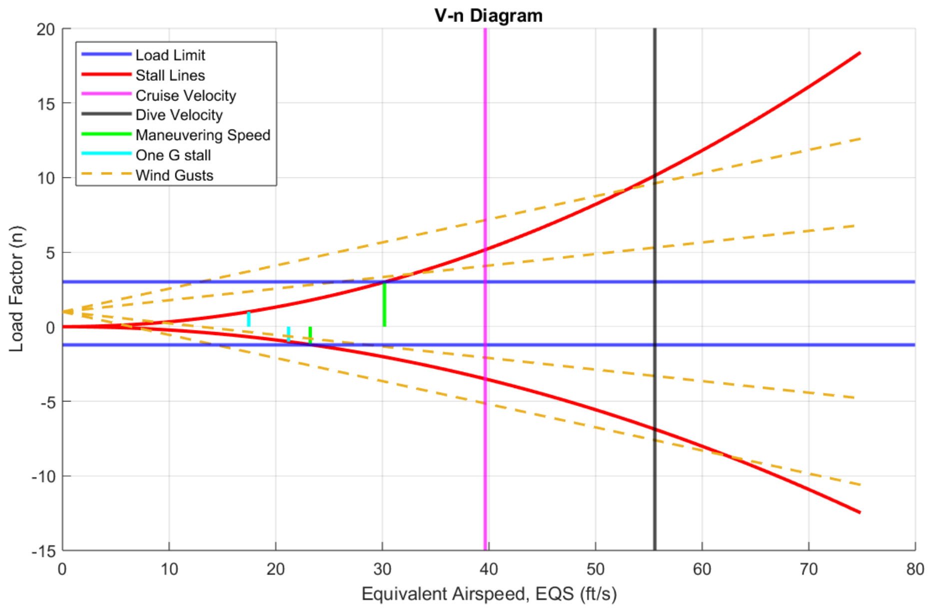

Figure 10: V-n Diagram for final design.

The above figure shows our v-n diagram. The cruise velocity and dive velocity are shown to be about 40 ft/s and 55 ft/s respectively. These values differ from our intended cruise velocity of 77 ft/s. The v-n dirham numbers are derived from the equations given to us and our wing loading, so we believe they indicate that our intended cruise velocity will suffer from wing flutter. When we begin our flight tests we will be sure to look out for flutter, but these values do not raise concerns about our actual cruise velocity. The diagram also shows how wind gusts of 25 and 50 ft/s will affect our aircraft and stall lines.

<u>Wing Load Analysis:</u>

Our team simplified our wing to the basswood strut, which serves as a cantilever beam. This additional simplification is highly conservative, as it assumes that the foam portion of the wing gives and the rear spar provides no structural support. The team used the equations below to calculate moment and displacement. We assume uniform area and moment of inertia for the entirety of the wingspan.

$$V = \int q dx \qquad M = \int V dx \qquad \Theta = \int M/EI dx \qquad D = \int \Theta dx$$

Assuming a cantilever beam, the wing tip has no shear and moment. Additionally, there is no deflection or angle at the root. The maximum bending and torsional loading conditions occur at the root. Maximum loading occurs during climb, and is approximated by the polyfit function below.

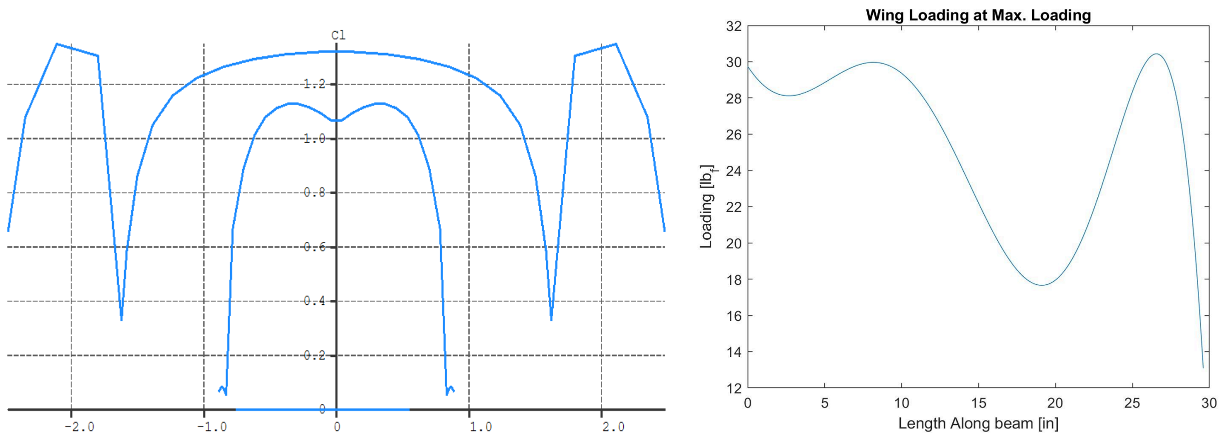

Figure 11: Wing loading from XFLR5 (left) and a MATLAB curve fit (right).

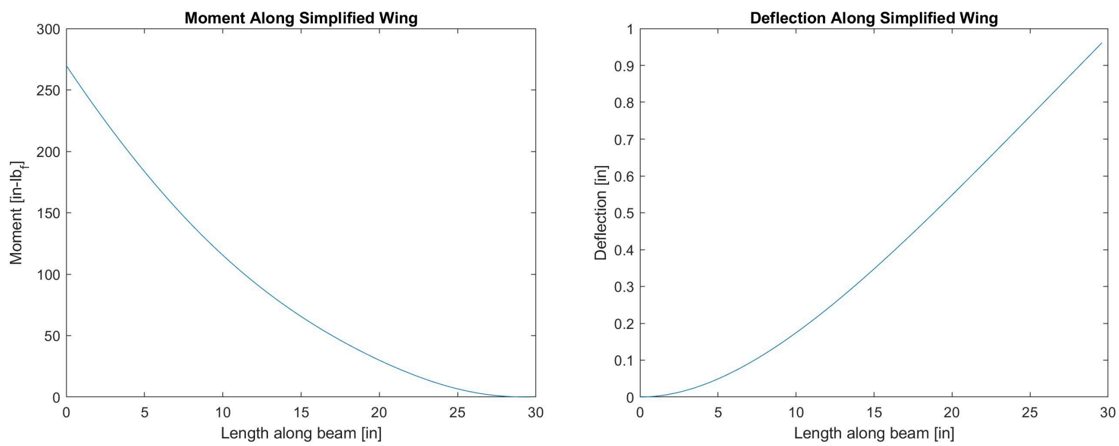

Figure 12: Moment and deflection along wing span.

At the wing root, there is a 270 in-lb moment. Assuming the moment occurs in the middle of the 1.25" spar, the max. compressive/tensile stress occurs 0.625" on the top/bottom of the spar. Using the moment equation $\sigma = - My/I$, the maximum stress is 3237 psi, which falls well within range for the 4730 psi compressive strength and 8700 psi bending strength.

The wing box comprises a 1"x1/2" basswood main spar at the ¼ chord and a 0.5"x1/8" balsa spar at the ¾ chord. The rear spar extends to the point where the ailerons begin. To ensure that the wing does not rotate by greater than 1 degree, the two spars are connected before the aileron by a piece of balsa. This will ensure limited rotation before the ailerons, which rotate depending on the control input. The basswood can conservatively handle 1.46 times the maximum wing loading shown above. This was calculated by dividing the compressive strength by the maximum root stress. The basswood can deflect about 1.4 inches before reaching compressive strength if this maximum loading occurs.

<u>Material Selection:</u>

For the fuselage, we are planning on using ⅛ inch thick balsa wood. Balsa wood is a light but relatively strong material, and is structurally sound enough to withstand aerodynamic forces. It is also relatively low in cost while also being easy to manufacture for our purposes. We will utilize ribs within the fuselage to keep the structure sound while also keeping weight low. We will also utilize one ½ inch by 1.25 inch rectangular wooden spar within the wing to increase stability of the wing itself. This will help counteract the critical loads placed on the wings and keep them safe. The tail will also utilize the spar that the wing does, and the vertical tail will not utilize extra structures to support loads.

For our wing, we will be using a NACA 2415 airfoil made of foam. This is low in cost and easy to manufacture. Based on past experiments using the foam, we will be reinforcing this material to make it stronger, which will be discussed later.

With regards to our tail, the horizontal stabilizer will be similar to the wing, but will be a NACA 0012 airfoil. For our vertical stabilizer, we will be using balsa wood again. We opted for balsa versus foam due to the fact that there will be a singular control surface, while the wing and horizontal stabilizer utilize two control surfaces. This means it needs to be more rigid for more controllability, and balsa wood is a better option because of this.

The wing-fuselage intersection for our high wing aircraft will utilize velcro and 2 rubber bands. A number of velcro strips will be placed on a 1/16 inch sheet of balsa wood above a divot at the top of the fuselage at the point of intersection. This divot will be deep enough to allow the leading edge and trailing edge of the airfoil to be flush with the top of the fuselage. These velcro strips will also be placed on the bottom of the airfoil at the point of intersection. These strips will be strong enough to keep the aircraft together during flight, but also allows for easy disassembly of the aircraft. In addition, we will utilize small pins on the sides of the fuselage to attach rubber bands in an x-shape, which will assist in keeping the airfoil attached to the fuselage.

The payload and battery will be placed between the nose and the leading edge of the airfoil. They will be placed within the fuselage, in a box large enough to carry both. This box will be closed by a small plank of balsa wood that will be held flush to the outer wall of the fuselage using velcro. This will allow for easy access as well as avoiding additional weight and cost.

Propulsion system

Process for Selection:

The main performance parameter that guided the selection process for our propulsion system was aiming for a thrust to weight ratio of around 1:1 after accounting for a 50% increase in total aircraft weight throughout the manufacturing process, which we will call out safety weight. This meant that, for an estimated aircraft weight of 7.672 lbf, our safety weight would be 11.508 lbf. The corresponding ideal thrust for a 1:1 thrust-to-weight ratio becomes 11.508 lbf.

Another major constraint that guided the process was hardware limitations in terms of battery selection. Most of the readily available and affordable hardware for RC aircraft (ESCs and motors) are compatible with LiPo batteries up to 6S cell configuration, thus setting an upper limit on the voltage the battery could provide.

Finally, using our constraint diagram, we needed to find a propulsion system capable of delivering enough mechanical power to satisfy our mission requirements. With a design power loading of 11.141 lbf/hp and using our safety weight, the calculated minimum mechanical power delivered to the propeller is equal to 1.032 hp.

Based on these 3 guiding selection principles, the final propulsion system components were chosen using eCalc, where we iterated through many components from common brands in order to satisfy these requirements, while trying to minimize both weight and cost. All calculations were made assuming an outside temperature of 40 F, what we expect to see during flight testing.

Selected System

Based on the requirements and constraints listed earlier, a battery was chosen that could deliver enough electrical power to the motor throughout the full length of the mission, plus a safety margin. The optimal battery turned out to be a Liperior 6S 3300 mAh, with a discharge rate of 30C and weight of 1.07 lbf. This battery is almost 3 times as heavy when compared to our initial estimate of 0.35 lbf based on historical data. Nonetheless, this tradeoff in weight means we are getting a lot more power and energy. Energy in Watt-hours is calculated as Wh = Voltage x Capacity, where Voltage = n x 3.7, where "n" is the number of cells in series, and capacity is in Ampere-hours (Ah). This results in a total energy stored of 73.26 Wh.

The propeller chosen is a 13in-diameter, 6.5in-pitch, 2-blade, APC Electric E propeller. The propeller is made out of injection-molded, long glass fiber composite with a nylon resin. The figures below show the performance parameters of the propeller as a function of advance ratio, at different rotational speeds. It is evident that, for all rotational speeds, the peak propeller efficiency occurs at an advance ratio of around 0.475. Moreover, the peak propeller efficiency is about 60%, which agrees with our initial guess that helped drive our constraint diagram.

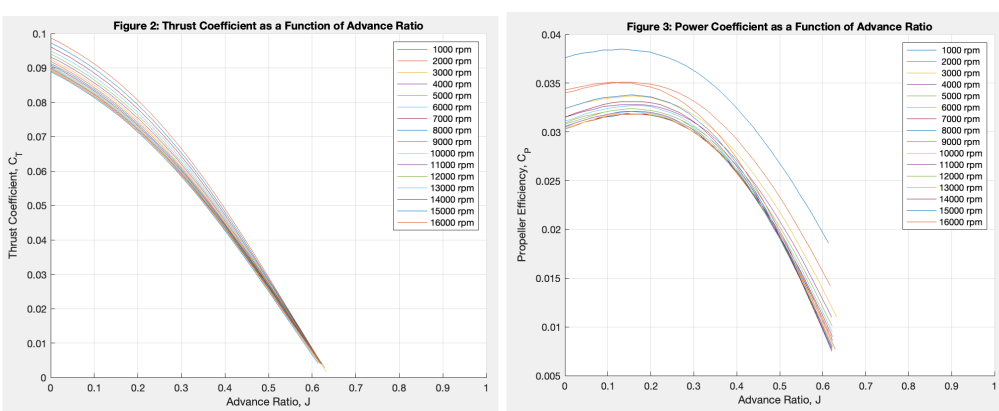

Figure 13: Thrust Coefficient vs Advance Ratio (Left) and Power Coefficient vs Advance Ratio (right)

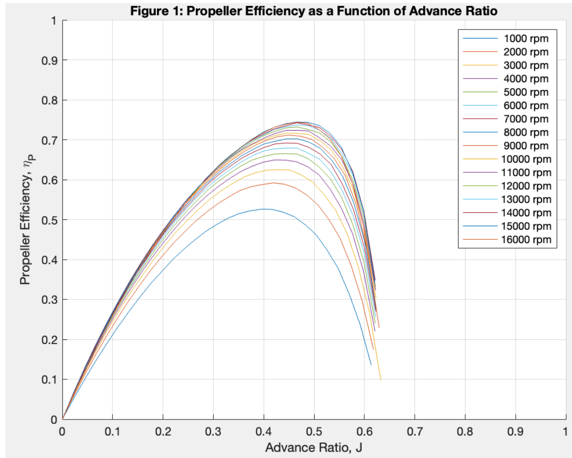

Figure 14: Propeller Efficiency vs Advance Ratio

The motor chosen to power our chosen propeller was a Cobra 4130/12 brushless motor. The motor's basic dimensions are an outer diameter of 1.961 in, and length of 2.433 in, with a total weight of 0.877 lbf. This motor can receive up to 1440 W of electrical power with a 6S battery, and is rated to a maximum continuous current of 65 A. The average motor efficiency is 91.6%, and the motor Kv is 540 RPM per volt.

Based on our mission requirements, thrust and power constraints, it was estimated that our best propulsion configuration drew 51.38 A of current at maximum performance. This meant that we needed an ESC capable of delivering at least 20% more than the max current draw, and supported a 6S LiPo battery. The chosen component was a RC Electric Parts 80A ESC.

The ESC chosen also outputs a BEC step down voltage of 5.5 at 4 amps. Our receiver and servos have a peak draw of 2.4 amps at this voltage, so our control systems will have ample power.

The component choices are summarized in the table below:

Battery	ESC	Motor	Propeller
Liperior 6S 3300 mAh 30C	RC Electric Parts 80A	Cobra 4130/12	APC 13x6.5E

Table 6: Propulsion system components.

Finally, all the major performance parameters are the following:

Parameter	Value
Energy [Wh]	73.26
Max Electric Power [hp]	1.400
Max Mechanical Power [hp]	1.282
Max Current Draw [A]	51.38
Static Thrust [lbf]	9.914
Thrust-to-weight Ratio	0.86
Max Flight Time [min]	4.8

Table 7: Propulsion system performance parameters.

Aerodynamics and Static Stability

Our aerodynamic analysis began with a component drag buildup using the methods presented in class. Our code that performs these calculations takes inputs from our defined concept geometry, the flight conditions, and the conceptual estimated weights for our aircraft. A test case was run to ensure proper performance of the code using the SR22 example from the lecture: the computed C_D from the lecture was 0.028, and the value found using our code was 0.02765 (this is a relative error of 1.25%). The code takes major components on an aircraft and estimates the experienced parasitic drag at some Reynolds number; it then adds this parasitic sum to an induced drag coefficient. The major components our code takes into account are the main wing, the horizontal and vertical tails, the fuselage, and any "miscellaneous" components, which the code estimates as 8% of the total parasitic drag coefficient. These components at cruise conditions gave us an estimated value for the parasitic drag and induced drag on our aircraft:

$$C_{D,o} = 0.0204,\ \ C_{D,i} = 0.00892$$

The code assumes no compressibility drag, which means our total estimated coefficient of drag is $C_D = 0.02934$. This value will be used later in XFLR5 to get a more complete overview of our aerodynamic performance. With drag estimated, we moved on to size our wing, tails, and fuselage, and control surfaces.

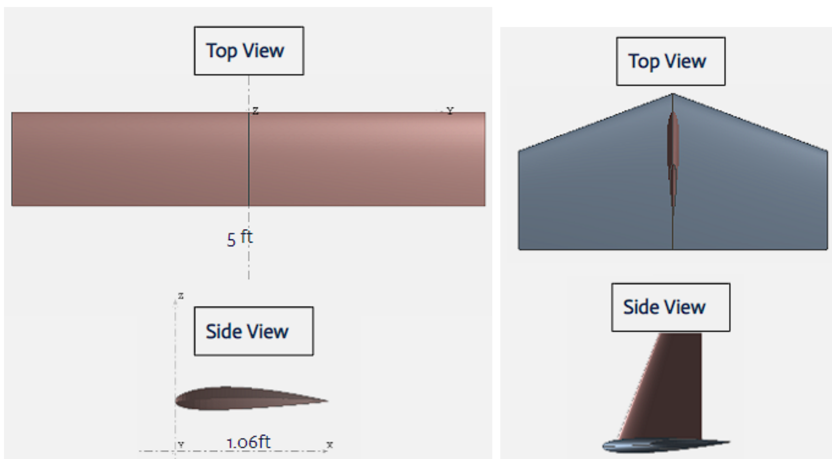

Figure 15: XFLR5 views of Wing (Left) and Tail (right).

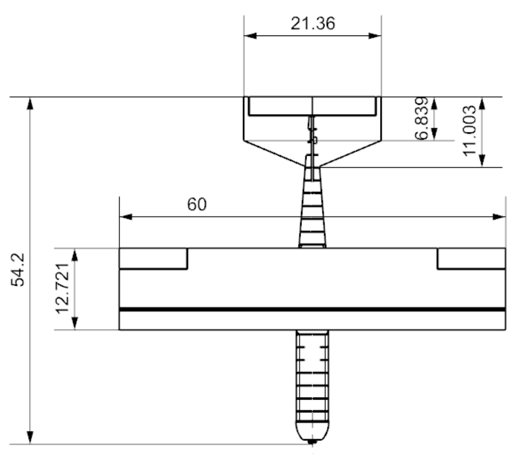

Figure 16: CAD top-down view of aircraft with relevant geometries labeled.

Our wing, tail, and fuselage sizing was all based on equations found in Raymer. The base of our geometric sizing comes from the following equation:

$$\textbf{Fuselage Length} = 3.5 * W_o^{0.23}$$

This equation is based on a singular variable, that being our aircrafts gross weight. At this stage in our design, we used our weight estimate from SRR+SDR using 4 units of payload: $W_o = 7.76\ lb_f$. We used an equation from Raymer for placement of our wing relative to the nose of our aircraft: 40% length of fuselage from the nose to the quarter chord of the wing. We used an equation to find the length from the quarter chord of our wing to the quarter chord of our tail 60% length of fuselage from the quarter chord of our wing to the quarter chord of our tail.

We ran multiple XFLR5 studies to determine optimal wing configurations, and after concerns of manufacturability were sourced to our aero team, we decided that an unswept, untapered wing with no dihedral would fit the overall requirements of the project while still achieving the desired performance. We also iterated through designs using different airfoils for our wings and tails, and we decided that the NACA 2415 for our wing and the NACA 0012 for our tails were adequate. Geometric sizing of our wing was rather simple; our constraint diagram from SRR+SDR gave us an estimate for our wing loading (W/S = 1.445), and using this along with our gross weight estimate we were able to solve for the geometry of our wing.

$$S_w = W_o / (W/S)$$

$$\text{Wing chord} = S_w / 5$$

We used estimates of tail volume coefficients to size our horizontal and vertical tail:

$$V_{Ht} = S_{Ht} * L_{Ht} / (S_w * c_w)$$

$$V_{Vt} = S_{Vt} * L_{Vt} / (S_w * b_w)$$

Our control surfaces were sized based on percentages of chord and span as given in lecture:

$$\text{Aileron chord} = 25\% * c_w, \text{ Aileron span} = 35\% * b_w$$

$$\text{Elevator chord} = 32.5\% * c_{Ht}, \text{ Elevator span} = 92.5\% * b_{Ht}$$

$$\text{Rudder chord} = 30\% * c_{Vt}, \text{ Rudder span} = 90\% * b_{Vt}$$

With following table provides a broad summary of the geometric properties of our aircraft:

Wing Area	5.32 ft^2	**Wing Span**	5 ft
Wing Chord	1.06 ft	**Wing Taper**	1 ($c_r = c_t$)
Horizontal Tail Mean Chord	0.76 ft	**Horizontal Tail Span**	1.78 ft
Horizontal Tail Area	1.35 ft^2	**Horizontal Tail Aspect Ratio**	2.35
Horizontal Tail Volume Coefficient	0.6	**Horizontal Tail Taper Ratio**	0.6 (c_r = 0.95 ft, c_t = 0.57 ft)
Vertical Tail Mean Chord	0.53 ft	**Vertical Tail Span**	0.80 ft
Vertical Tail Area	0.42 ft^2	**Vertical Tail Aspect Ratio**	1.5
Vertical Tail Volume Coefficient	0.04	**Vertical Tail Taper Ratio**	0.65 (c_r = 0.95 ft, c_t = 0.57 ft)

Fuselage Length	4.2 feet	**Fuselage Diameter**	10 inches

Table 8: Geometric summary for aerodynamic surfaces.

Aileron Span	1.75 ft	**Aileron Chord**	0.266 ft
Elevator Span	1.65 ft	**Elevator Chord**	0.247 ft
Rudder Span	0.72 ft	**Rudder Chord**	0.159

Table 9: Control Surface geometries.

With our geometry and weights well defined, we were ready to generate aerodynamics plots and run stability tests using XFLR5. To better account for drag, we input our drag values and areas as calculated in our drag buildup. Our primary focus was to understand cruise performance, so we ran multiple fixed lift simulations to determine an ideal trim velocity.

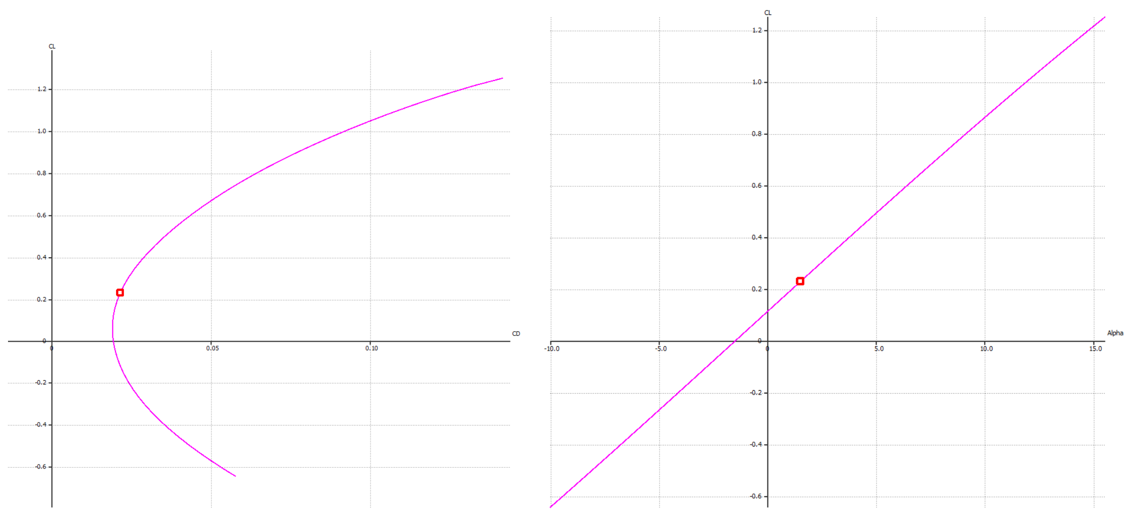

Figure 17: XFLR5 plots of Drag Polar and C_L vs. Alpha for a 77 ft/s fixed speed simulation.

Using an XFLR5 fixed lift simulation with our aircraft weights, geometries, and extra drag surfaces included, we found our aircraft was longitudinally stable as it had a negative C_m vs alpha curve and a positive C_{mo}. We found our trim angle of attack at cruise and its associated trim velocity to be 1 degree and 77 ft/s respectively. The trim cruise velocity is close to our original value used for sizing in SRR+SDR of 70 ft/s. With our trimmed cruise speed finalized, we ran fixed speed simulations to obtain the figures shown directly above and below. All analyses were run using the Ring Vortex method in XFLR5 (vortex latus method 2).

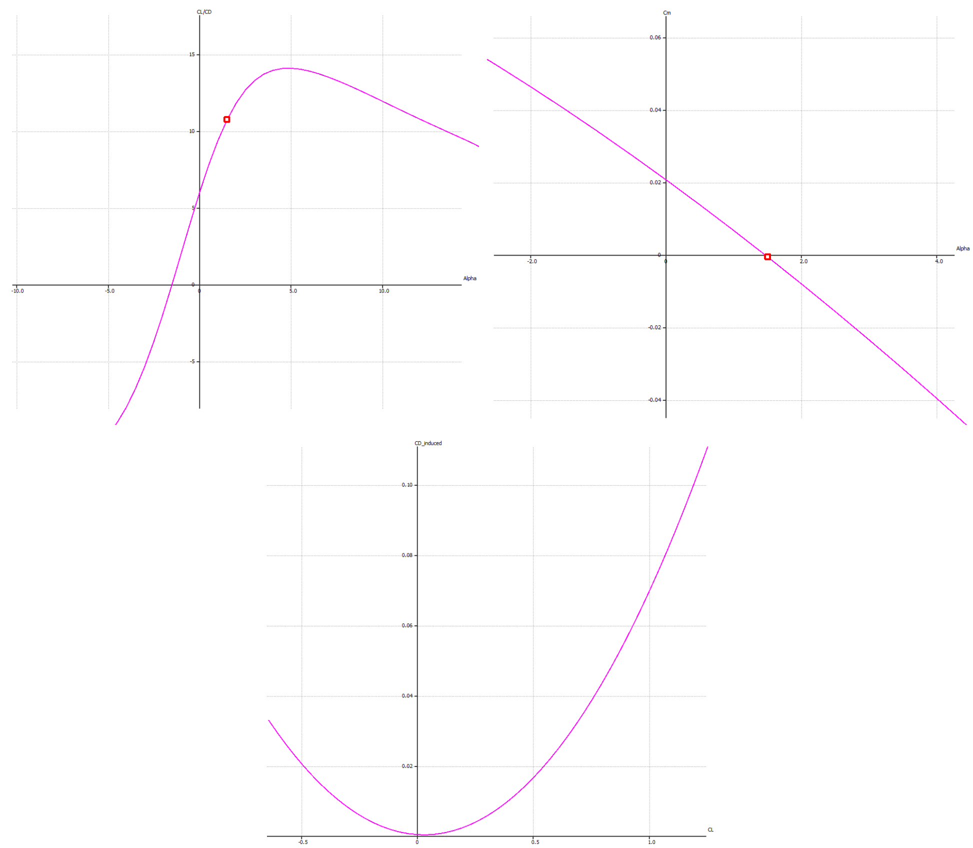

Figure 18: XFLR5 Plots of L/D, C_m vs. AoA, and Induced Drag vs. C_L for a 77 ft/s fixed speed simulation.

With our configuration and our center of gravity known, we were able to determine our static margin. Using a neutral point value of 0.505 ft aft of the leading edge obtained using XFLR5:

$$\mathbf{SM = (x_{NP} - x_{CG}) / c = 18.5\%}$$

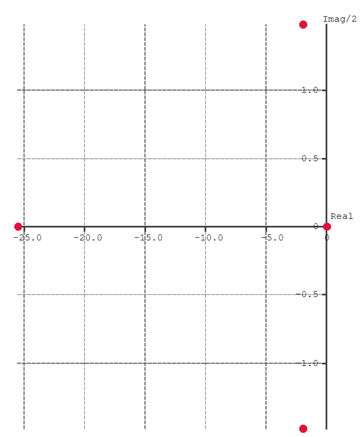

Figure 19: Root Locus for stability analysis on aircraft.

Our root locus from XFLR5 shows that all our eigenvalues have negative real components, further proving the stability of our aircraft.

Dynamics and control

Servo Sizing

The servos are sized such that a 30 degree deflection in the angle on the servo arm will translate to a 25 degree deflection of the control surface it is attached to, allowing for ±25 degree deflection on the ailerons, rudder, and elevator. We intend to use one HS-311 servo to control the elevator and 3 EMAX ES08MA II servos to control each aileron and the rudder.

Servo	Count	Stall Torque (oz-in)	Weight (oz)	Max Current (mA)	Voltage (V)	Cost per Servo ($)
HS-311	1	42-49	1.51	800	4.8 - 6	13.49
EMAX ES08MA II	3	21-28	0.42	500	4.8 - 6	7.75

Table 10: Servo Specifications

Additional Control Components

We also had to purchase control horns, linkages, servo extenders, and hinges as part of the control system. Hinges will be used to attach the ailerons to the wings and rudder and elevator to tail. The control horns and linkages will connect the control surfaces and servos. Finally the extenders are used to connect the servos to the receiver. Our extenders will be 3 feet long, long enough to connect the servos to the receiver under the wing connection with a margin of safety in case we decide to move the receiver's internal position.

Control Authority

To analyze control authority, we used XFLR5 to analyze performance under cruise conditions with deflected control surfaces. Even though we plan to have elevator deflection of ±25 degrees, we had trouble getting convergence past -15 degrees, so the following plots show -15, 0, and 25 degree elevator deflection in red, green, and blue respectively.

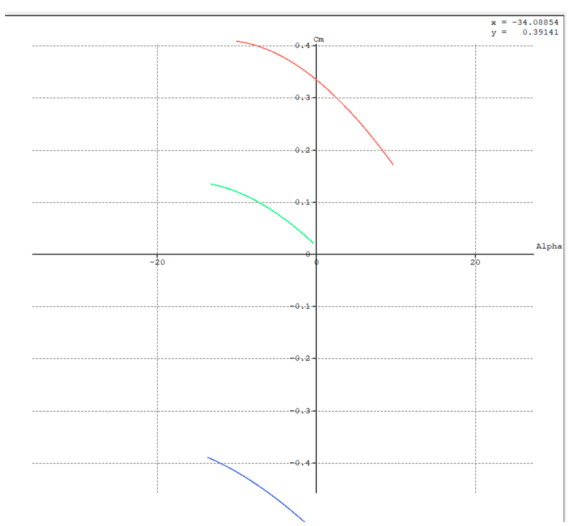

Figure 20: Moment Coefficient vs Angle of Attack

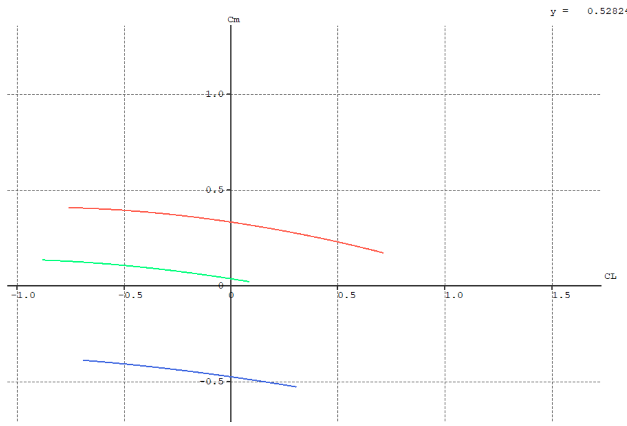

Figure 21: Moment Coefficient vs Coefficient of Lift

These plots are not complete because of convergence issues, however we believe if we could get a full line placed for the elevator in the -25 degree position, that it would show a lift coefficient greater than 1.2 when the moment coefficient is equal to 0. This would mean that we could reach our max lift coefficient and stall the aircraft. Our lift coefficient at cruise is 0.2, and it looks like if our elevator has a slight negative deflection then Cl would equal 0.2 at Cm = 0. These conditions fulfill control authority.

Flight Performance

Takeoff

We estimate that one of our team members can lightly jog at 10 ft/s and throw an object vertically upward at 2 ft/s from an initial height of 6 feet (roughly head height). With these initial conditions in mind and our aircraft's aerodynamic data known from XFLR5, we were able to run a dynamic simulation using ODE45 to determine the trajectory of our aircraft at takeoff.

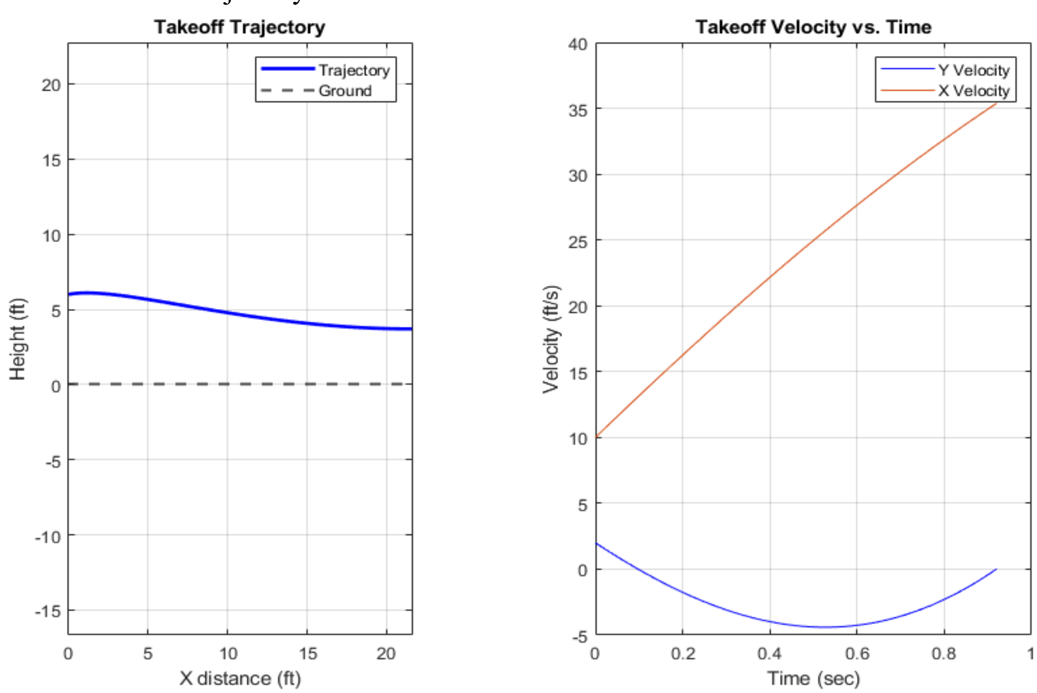

Figure 22: ODE45 simulation results for takeoff.

We used a rough estimate of the equations of motion for an aircraft at takeoff, as well as our takeoff thrust provided by eCalc to complete this simulation.

$$F_x = \text{Thrust} * \cos(\text{alpha}) - \text{Lift} * \sin(\text{alpha}) - \text{Drag} * \cos(\text{alpha})$$
$$F_y = \text{Thrust} * \sin(\text{alpha}) + \text{Lift} * \cos(\text{alpha}) - \text{Drag} * \sin(\text{alpha})$$
$$V = \text{sqrt}(V_x^2 + V_y^2) \quad \text{and} \quad \text{alpha} = \tan^{-1}(V_y / V_x)$$

An important caveat for these results is that the coefficients of lift and drag were constants and not functions of the changing angle of attack. This simulation was run until the Y component of velocity was no longer negative. This occurred after 0.92 seconds of flight, at which point for the sake of our flight test we will consider the takeoff segment of the mission to be completed and the climb segment to be started. Using XFLR5, we ran a fixed speed simulation at the final takeoff velocity (48.5 ft/s) to determine parameters of interest at the end of our takeoff segment. This simulation was run with elevator deflection set to 25 degrees down and aileron deflection at 20 degrees down. This configuration gives us a coefficient of lift of 1.4 at an AoA14 degrees, which is the initial angle we will be targeting to throw our aircraft.

C_L	C_D	L/D	C_m	AoA	V
0.599	0.116	5.16	-0.595	0 deg	48.5

Table 11: Performance values at the end of takeoff.

We can tabulate our aircrafts dimensionalized lift, drag, and thrust available at takeoff using the following equations:

$$\text{Lift} = C_L \, q_{inf} \, S_{ref}$$
$$\text{Drag} = C_D \, q_{inf} \, S_{ref}$$
$$q_{inf} = ½ * V^2 * \rho$$
$$\text{Thrust Available} = \text{Maximum Thrust} - \text{Drag}$$

Plugging in our known values gives the following dimensionalized aerodynamic forces and thrust available:

Lift	Drag	Thrust Available
8.93 lb_f	1.729 lb_f	7.62lb_f

Table 12: Dimensionalized Lift and Drag and Thrust available at takeoff.

At takeoff, we will be relying on our oversized propulsion system, in other words we know that we will not be able to reach our stall speed before crashing into the ground (as can be seen from our dimensionalized lift value above being less than our aircrafts weight). We will seek to maintain an angle of attack close to that of our climb AoA so that our high thrust can be utilized to create upwards acceleration. That being said, the thrust available value above of 9.13 lb_f is misleading with the newfound context of our mission; we will be using our maximum thrust at takeoff and thus will have no extra “available” thrust during our takeoff mission segment.

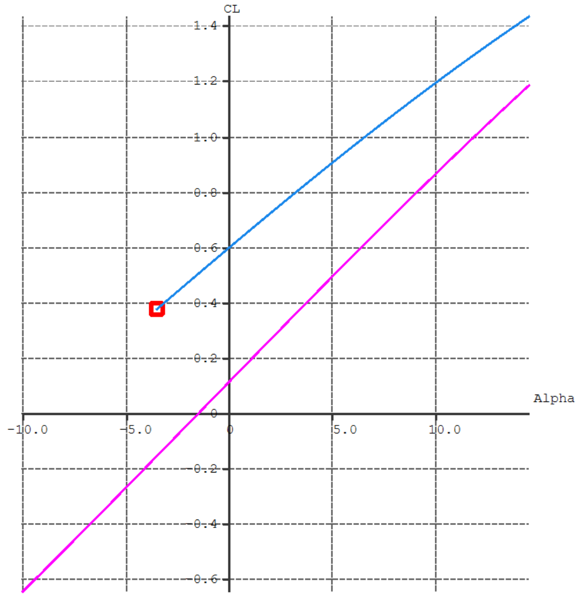

Figure 23: C_L vs. Alpha curve for aircraft with no deflection (purple curve) and max lift deflections (blue curve)

Climb

We struggled with non-converging simulations above 15 degrees using our completed aircraft configuration in XFLR5, therefore we have decided to change our climb angle to 15 degrees rather than the 20 degrees previously discussed in our SRR+SDR report. We decided that a 25 degree aileron and elevator control surface deflection was adequate for climb. Running an XFLR5 simulation with these conditions at a fixed speed of 55 ft/s gave the following performance parameters:

C_L	C_D	L/D	C_m	AoA	V
1.41	0.291	4.84	-0.774	15 deg	55 ft/s

Table 13: Performance values during climb.

With these parameters now known, we were able to determine our dimensionalized Lift and Drag values during climb (using the same equations as takeoff):

Lift	Drag	Thrust Available
26.83 lb_f	5.615 lb_f	3.74 lb_f

Table 14: Dimensionalized Lift and Drag and Thrust available at climb.

The last performance metric we wanted to find for the climb duration of our mission was our rate of climb. We felt that the easiest way to solve for this value was to use trigonometry. A right triangle can be created from our takeoff trajectory; the hypotenuse is our climb velocity (estimated to be 55 ft/s), and the angle between the horizontal and hypotenuse is our flight path angle AoA (15 degrees). Using this method, we estimate our rate of climb to be 14.24 ft/s. Assuming we climb to an altitude of 200 ft, this means our climb duration will be 14.05 seconds. Our group has concerns with determination of altitude during flight tests, and thus we will not seek to optimize flight performance as a function of altitude. That being said, our climb will stop at an altitude 200 ft at which point we will consider our aircraft to be at a cruising altitude.

Cruise

Our aircraft's cruise velocity was determined in the aerodynamic section of this report to be 70.247 ft/s. Running a fixed speed simulation in XFLR5 gave the following performance outputs:

C_L	C_D	L/D	C_m	AoA (trimmed)	V
0.1919	0.0362	5.38	0	1 deg	77 ft/s

Table 15: Performance values at cruise.

As done previously, we can find our dimensionalized lift, drag, and our thrust available at cruise:

Lift	Drag	Thrust Available
7.208 lb_f	1.36 lb_f	7.99 lb_f

Table 16: Dimensionalized Lift and Drag and Thrust available at cruise.

Turning

Turns for this mission had a radius of 100 ft as specified by the RFP. To start our analysis of our turning flight, we decided to deflect our ailerons by 15 degrees in opposite directions on either wing along with a 15 degree deflection of our rudder to initialize a right turn (positive yaw with z axis pointing down). What followed was an iterative process to select a sideslip angle for our turns. We ran multiple fixed lift simulations until we found a value for beta that gave us a trimmed velocity (zero moment coefficient) of 65 ft/s. We found that a sideslip of 15 degrees at an angle of attack of 2.25 degrees gave us a trimmed velocity of 65.67 ft/s. With these turning variables noted, we were able to obtain aerodynamic data for our aircraft turns:

C_L	C_D	L/D	C_m	AoA (trimmed)	V
0.2629	0.067	3.92	0	2.25 deg	65.67 ft/s

Table 17: Performance values during turns..

As done previously, we can find our dimensionalized lift, drag, and our thrust available during turns:

Lift	Drag	Thrust Available
7.208 lb_f	1.83 lb_f	7.52 lb_f

Table 18: Dimensionalized Lift and Drag and Thrust available during turns.

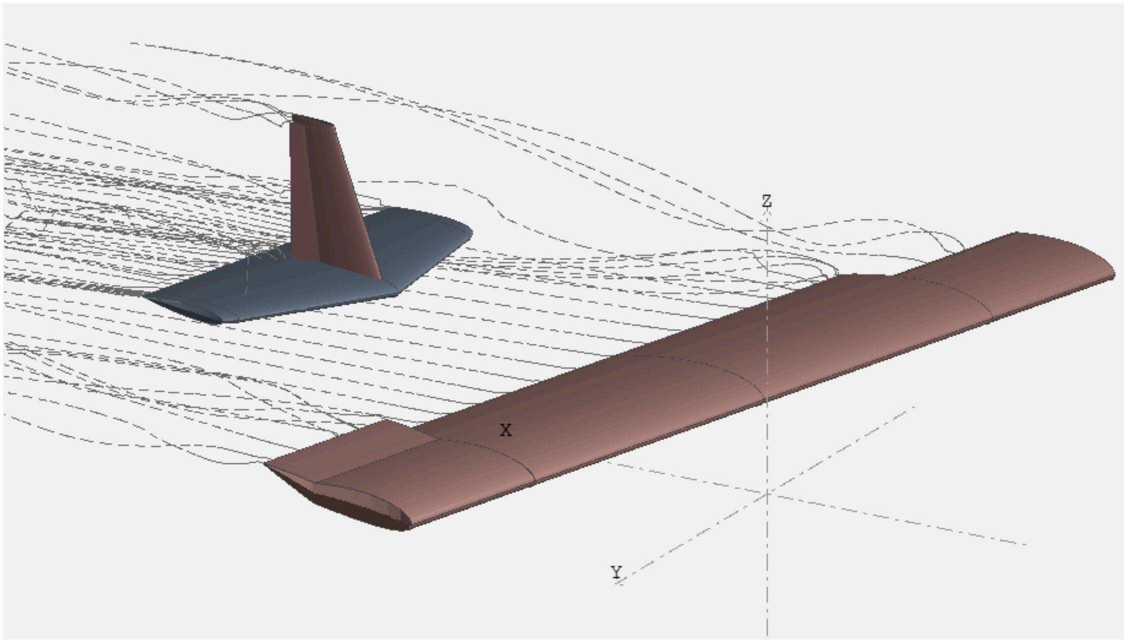

Figure 24: Turning flight control surface layout with streamlines featured.

Time of Flight:

Without our mission velocities known and our flight path distance given in the RFP, we were able to breakdown the time in each mission stage:
Takeoff → 0.92 sec, Climb → 14.05 sec, Cruise → 51.51 sec, Turns → 26.93 sec.

Parts Acquisition List

The parts acquisition list is listed in the figure below:

Part Name	Description
Cobra C-4130/12 Brushless Motor, Kv=540	Motor
Cobra 60A ESC with 6A Switching BEC	ESC
Liperior 3300mAh 6S 30C 22.2V Lipo Battery	Battery
13x6.5E	Propeller
HS-311 Servo-Stock Rotation	Servo
EMAX ES08MA II	Servos
FOAMULAR NGX F-250 2 in. x 4 ft. x 8 ft. SSE R-10 XPS Rigid Foam Board Insulation	Foam
National Balsa	Balsa Wood
Large Size Nylon Pinned Hinges	Hinges
36" Servo Extenders	Servo Wires
Velcro Alfalock	Velcro
HobbyPark 20pcs Nylon Control Horns	Control Horns and Linkages
Nose Cone	3D-Printed Nose Cone
SPAX® #6 x 1-3/4" Combo Drive Zinc Flat Head Wood Screw - 25 Count	Screw
Hillman #6 x 32 Zinc-plated Steel Hex Nut (24-Count)	Nut
8 oz. Wood Glue/Epoxy	Glue
Monocoat	Monocoat
Rubberbands	Rubber bands
Velcro	Velcro payload

Figure 25: Parts List

The figure shows all of the materials and items we will need to acquire for the complete construction of our aircraft. This includes components of the propulsion and control system, along with structural components including foam and woods, and items used to keep the plane together such as glue and velcro. The links to these suppliers are listed in the appendix below.

Prototype fabrication, economic, and test plan

The project will follow a defined schedule detailing the timeline for each component's manufacture and testing. Firstly, CDR must be completed by Wednesday October 9th. Secondly, after the completion and presentation of CDR and contingent on the design's acceptance, parts ordering must be accomplished by Monday October 21st.

Following these milestones the manufacturing process will follow the gantt chart schedule shown below in Figure 26:

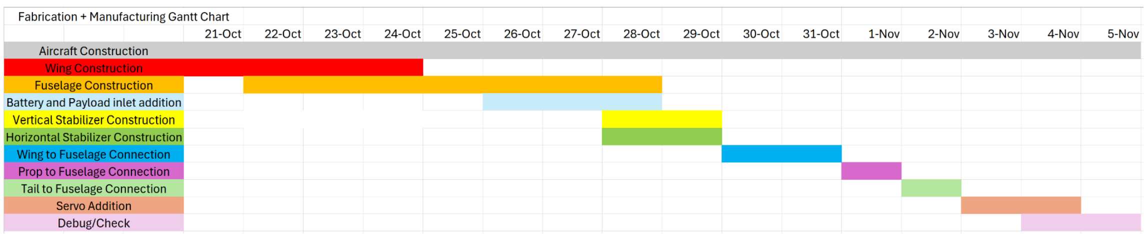

Figure 26: Manufacturing Schedule

The manufacturing process is as follows; the wings will be cut out of XPS foam using the foam cutter in the lab. We will cut not only the airfoil out of the stock but also cut the channel in which our spar will sit. The horizontal stabilizer will also utilize the foam cutter and be made of the same XPS foam. In addition to the foam cutter we will cut the inward facing ends of the horizontal stabilizer as required in order to fit them through the ribs at the tail of our fuselage and secure them onto a rod connecting the two halves of the horizontal stabilizer to each other, the tail of the fuselage, and the vertical stabilizer. The vertical stabilizer will be made of balsa and will be laser cut to the desired shape from a sheet of stock. This laser cutting process will also cut the hole for the rod as well as the slits which allow it to fit into and fasten to the tail of the fuselage. The fuselage will be built using laser cut pieces of balsa which will form the ribs and horizontal structural beams. These ribs will be notched to allow them to easily fit onto the beams and glue will be used to secure their position. A layer of monocoat will be used to cover the fuselage and provide an aerodynamic skin around the ribs. A nose cone will be 3D printed and used to help secure the motor to the fuselage. A small curved block will also be 3D printed which will act as the connection surface where the wing will be fastened to the fuselage via velcro. Additionally the control surfaces will be made of the same material as their main component. The control surfaces will be hand cut from their main component and be trimmed such that hinges can be attached to guide rotation. The servos will be housed within the foam airfoils by carving out the needed space and gluing them in place. Additional channels will be cut where necessary to allow the wiring to traverse as necessary. Tape will be used to cover the carved channels for the wiring, to cover the cuts of the control surfaces, and for the channel in which the spar runs.

The order of assembly will be to first assemble the fuselage. This involves gluing the ribs to the horizontal beams and applying the monocote skin to the exterior. Then the small curved block will be glued to the interior ribs and extrude through a hole in the monocoat. The nose cone will then be attached to the fuselage via four bolts with a nut and washer on the interior of the fuselage. These bolts will also fasten the motor to the fuselage. Additionally glue the ESC to the top of the fuselage and poke a hole for the required wiring in the monocoat.

The next step is to attach the cut vertical stabilizer onto the fuselage by joining the cut slits of the vertical stabilizer with the ribs of the fuselage. Then the rod is placed through the fuselage and vertical tail. Additionally, glue will be added to the seams as necessary.

The cut horizontal stabilizer is then added in a similar manner to the vertical stabilizer. Join the cut sections of the stabilizer to the ribs of the fuselage and onto the rod then glue as necessary. Next attach the battery, receiver, and payload to the interior of the fuselage via velcro squares and wire as needed.

The next step is to attach velcro to the 3D printed curved portion of the fuselage and the opposing surface of the wing which contacts that surface. After the adhesive settles the two sections can be connected and rubber bands can be stretched across the top surface of the wing in an "X" shape and be hooked onto the extruding pins from the fuselage.

Finally attach the servo to the control surface via a linkage to a nylon horn which is glued to the subsequent control surface.

The cost breakdown is shown below in Figure 27. The cost is broken down by individual components and location ordered from.

Part Name	Supplier	Total Cost ($)
Cobra C-4130/12 Brushless Motor, Kv=540	Cobra	$87.99
Cobra 60A ESC with 6A Switching BEC	Amazon	$37.49
Liperior 3300mAh 6S 30C 22.2V Lipo Battery	RC Battery	$46.99
13x6.5E	APC Propellers	$5.73
HS-311 Servo-Stock Rotation	Servo City	$13.49
EMAX ES08MA II	EMAX	$23.25
FOAMULAR NGX F-250 2 in. x 4 ft. x 8 ft. SSE R-10 XPS Rigid Foam Board Insulation	Home Depot	$46.48
National Balsa	Balsa Wood	$31.44
Large Size Nylon Pinned Hinges	Amazon	$8.99
36" Servo Extenders	Amazon	$17.99
Velcro Alfalock	Amazon	$6.68
HobbyPark 20pcs Nylon Control Horns	Amazon	$8.97
Nose Cone	3D Print	$1.00
SPAX® #6 x 1-3/4" Combo Drive Zinc Flat Head Wood Screw - 25 Count	Lab	$3.10
Hillman #6 x 32 Zinc-plated Steel Hex Nut (24-Count)	Lab	$1.48
8 oz. Wood Glue/Epoxy	Home Depot	$4.97
Monocoat	Amazon	$16.99
Rubberbands	Lab	$1.00
Velcro	Amazon	$3.50
Total Cost	**$367.53**	

Figure 27: Cost Breakdown by Component

Following the manufacturing process we plan to conduct two tests in order to establish the airworthiness of our design. Firstly upon completion of manufacturing the team will hold an unpowered glide flight test in Lambert fieldhouse to test the airworthiness of our design. The team will both hand throw the aircraft from ground level to test not only the glide distance but also to test the weight and human launch aspect that will be present in the final flight. Next the team will launch the aircraft from the second story balcony to further test the gliding capability. This will be done secondly as the increased height comes with an increased risk of damage if the aircraft is unsuccessful.

The second test we will complete is a static test of our propulsion and control surfaces. We will statically hold the aircraft and test the propulsion at the different levels of thrust that the craft will face in flight. We will also actuate the control surfaces to verify that they are both responsive and actuate to the degree required.

Appendix

Code:
AAE451_SeniorDesign

XFLR5:
HighWing.xfl

Part Acquisition List (with links):

Part Name	Description	Supplier
Cobra C-4130/12 Brushless Motor, Kv=540	Motor	Innov8tive Designs
Cobra 60A ESC with 6A Switching BEC	ESC	Amazon
Liperior 3300mAh 6S 30C 22.2V Lipo Battery	Battery	RC Battery
13x6.5E	Propeller	APC Propellers
HS-311 Servo-Stock Rotation	Servo	Servo City
EMAX ES08MA II	Servos	EMAX
FOAMULAR NGX F-250 2 in. x 4 ft. x 8 ft. SSE R-10 XPS Rigid Foam Board Insulation	Foam	Home Depot
National Balsa	Balsa Wood	Balsa Wood
Large Size Nylon Pinned Hinges	Hinges	Amazon
36" Servo Extenders	Servo Wires	Amazon
Velcro Alfalock	Velcro	Amazon
HobbyPark 20pcs Nylon Control Horns	Control Horns and Linkages	Amazon
Nose Cone	3D-Printed Nose Cone	3D Print
SPAX® #6 x 1-3/4" Combo Drive Zinc Flat Head Wood Screw - 25 Count	Screw	Lab
Hillman #6 x 32 Zinc-plated Steel Hex Nut (24-Count)	Nut	Lab
8 oz. Wood Glue/Epoxy	Glue	Home Depot
Monocoat	Monocoat	Amazon
Rubberbands	Rubber bands	Lab
Velcro	Velcro payload	Amazon